

This is the accepted manuscript made available via CHORUS. The article has been published as:

## Unified Formalism of Andreev Reflection at a Ferromagnet/Superconductor Interface

T. Y. Chen, Z. Tesanovic, and C. L. Chien

Phys. Rev. Lett. **109**, 146602 — Published 3 October 2012

DOI: [10.1103/PhysRevLett.109.146602](https://doi.org/10.1103/PhysRevLett.109.146602)

# Unified formalism of Andreev reflection at a ferromagnet/superconductor interface

T. Y. Chen<sup>1</sup>, Z. Tesanovic<sup>2\*</sup>, and C. L. Chien<sup>2</sup>

<sup>1</sup>*Department of Physics, Arizona State University, Tempe 85287, USA*

<sup>2</sup>*Department of Physics and Astronomy, Johns Hopkins University, Baltimore, MD 21218, USA*

## Abstract

We present a unified formalism of Andreev reflection of a partial polarized current at a ferromagnet/superconductor interface instead of assuming a linear combination of unpolarized and polarized currents. The Andreev reflection is limited by the states of minority spins and the extra majority spins become evanescent wave. We further study the effects of spin polarization, inelastic scattering, and interfacial scattering on the Andreev reflection, normal reflection, and transmitted probabilities in equilibrium as well as under a bias. Our model, which reduces to those of BTK, Mazin, and Dynes models in three limiting cases, provides a significantly better description of the experimental results.

The spin polarization  $P$  of a ferromagnet (FM), defined as the imbalance of the normalized density of states (DOS) of the majority and the minority spins at the Fermi level, plays a pivotal role in many magnetoelectronic phenomena, including giant magnetoresistance, tunneling magnetoresistance (TMR), and spin torque effects. Yet, the value of  $P$  is often the least known, in part because only a few methods can measure  $P$ . Spin-polarized photoemission studies, highly susceptible to surface states and contamination, have reported  $P$  values of 0% [1] and 100% [2] for Ni, both are far from the actual value of  $P \approx 40\%$ . Spin dependent tunneling, including  $F_1/I/F_2$  and  $F/I/S$  junctions, depends stringently on the quality of the insulator ( $I$ ) barrier. The TMR value of nominally the same  $F_1/I/F_2$  junctions could vary by orders of magnitude [3-5].

Andreev reflection (AR) has been extensively used to measure the  $P$  values of many FMs [6-25]. At a normal metal/superconductor ( $NM/S$ ) interface within the superconducting gap, a normal current must be converted into a supercurrent, where an electron is accompanied by another of the opposite spin. This is equivalent to a hole reflected back into the normal metal, the essential AR process, thus doubling the conductance within the gap. In contrast, at a half-metal/superconductor ( $HM/S$ ) interface, the said conductance is zero due to the absence of electrons with the opposite spin. With quantitative analyses, one can determine  $P$  of FMs as well as the superconducting gaps using AR spectroscopy [26].

The classic Blonder-Tinkham-Klapwijk (BTK) model [27] and the Mazin model [28, 29] quantitatively describe AR of a fully unpolarized current at a  $NM/S$  interface and a fully polarized current at a  $HM/S$  interface respectively. Most FMs are partially polarized with  $P$  between 0 and 1. Previously, the only available option is the linear model where one *assumes* a *linear* combination of a fully unpolarized current (the BTK model) and a fully polarized current

(the Mazin model) with the spin polarization  $P_I$  as the coefficient,  $I = I(1 - P_I) + IP_I$ . This linear relation may be valid for transparent interfaces, but questionable at non-transparent interfaces. Inelastic scattering in superconductors ( $N/I/S$ ) and ( $S/I/S$ ) junctions has been successfully incorporated using an imaginary component to the energy within the Dynes model [30] and has also been included in the BTK model for an unpolarized current [31] but not for a fully polarized current.

In this work, we provide a unified description of the AR at F/S interfaces valid for arbitrary polarization that encompasses the BTK and the Mazin models *without* assuming a linear combination. In our model, AR is limited by the minority spins while the redundant spin of the majority becomes evanescent. The spin polarization is naturally included and, most importantly, the effects of spin polarization, inelastic and interfacial scattering can now be studied for all the probabilities involved in the AR process. Our unified AR model reduces to the BTK, the Mazin and the Dynes models in the three limiting cases. We show that the value of  $P$  is substantially different from  $P_I$  of the linear model except when the interface is transparent. We demonstrate that our general model provides a better description of the experimental data, especially at low bias.

We consider a partially-polarized current at an F/S interface in equilibrium. The incident

and transmitted plane waves are  $\psi_{inci} = \begin{pmatrix} 1 \\ 0 \end{pmatrix} e^{iq^+x}$ ,  $\hbar q^\pm = \sqrt{2m(\mu \pm E)}$ ,

$\psi_{trans} = c \begin{pmatrix} \tilde{u} \\ \tilde{v} \end{pmatrix} e^{ik^+x} + d \begin{pmatrix} \tilde{v} \\ \tilde{u} \end{pmatrix} e^{-ik^-x}$ , where  $\tilde{u}$  and  $\tilde{v}$  are the BCS complex coherence factors,

$\tilde{u}^2 = 1 - \tilde{v}^2 = (1 + \sqrt{(|E| + i\Gamma)^2 - \Delta^2} / (|E| + i\Gamma)) / 2$ , in which  $\Gamma$  is the inelastic scattering factor,  $E$  is the quasi-particle excitation energy above the ground state ( $E \geq 0$ ). The wave vectors are defined as

$\hbar k^\pm = \sqrt{2m(\mu \pm E)}$  and  $\hbar q^\pm = \sqrt{2m(\mu \pm \sqrt{E^2 - \Delta^2})}$ . The effect of mismatch of Fermi vectors can be attributed to the  $Z$  factor [27]. Here since  $\mu \approx E_F \gg E$  and  $E_F \gg \Delta$ , for simplicity we take  $k^\pm \approx q^\pm \approx k_F$ . The reflected wave function including normal reflection, AR, and evanescent wave is  $\psi_{refl} = a \begin{pmatrix} 0 \\ 1 \end{pmatrix} e^{(\alpha+i)q^-x} + b \begin{pmatrix} 1 \\ 0 \end{pmatrix} e^{-iq^+x}$ , where  $\alpha$  is a dimensionless real number. In analogy to total internal reflection,  $\alpha$  represents the portion of evanescent wave. When  $\alpha \neq 0$ , the boundary conditions generically remain the same because the evanescent wave does not contribute to the current. These boundary conditions demand continuity of the wave function and compel its derivative to satisfy the potential function  $H\delta(0)$  at the interface.

The calculated coefficients  $a$ ,  $b$ ,  $c$  and  $d$  are listed in Table I (1<sup>st</sup> row) and depend on  $\alpha$ ,  $E$ ,  $Z$ , and  $\Gamma$ .  $Z \equiv \frac{mH}{\hbar^2 k_F}$  represents the interfacial scattering. The probabilities of Andreev  $A = aa^*$  and normal reflections  $B = bb^*$  can then be evaluated straightforwardly. Similarly, the transmitted probability without-branch-crossing  $C$  and with-branch-crossing  $D$  are  $C = cc^*(\tilde{u}\tilde{u}^* - \tilde{v}\tilde{v}^*)$  and  $D = dd^*(\tilde{u}\tilde{u}^* - \tilde{v}\tilde{v}^*)$ , where  $\tilde{u}\tilde{u}^* - \tilde{v}\tilde{v}^*$  is the group velocity. The probability is manifestly conserved with  $A + B + C + D = 1$  for any real  $\alpha$ , consistent with the boundary conditions.

When  $\alpha = 0$ , the coefficients are exactly those of the BTK model [27] for an unpolarized current, as shown in Table I (2<sup>nd</sup> row). One notes that, by introducing the generalized complex BCS coherence factors  $\tilde{u}$ ,  $\tilde{v}$  and the group velocity  $\tilde{u}\tilde{u}^* - \tilde{v}\tilde{v}^*$ , we have already included the effect of inelastic scattering. When  $\alpha = \infty$ ,  $a$  is zero and  $b$ ,  $c$ ,  $d$  are reduced for a fully polarized current listed in Table I (3<sup>rd</sup> row). Previously,  $b$ ,  $c$  and  $d$  for a polarized current have not been

calculated and only the probability  $B = bb^*$  has been given by the Mazin model. A simple calculation of the normal reflection from Table I shows that  $B$  is exactly the expected result for a fully polarized current [28].

In the BTK model, when  $Z = \infty$ , the Andreev spectrum becomes the tunneling spectrum, the DOS of the superconductor. In our model with the inelastic effect and spin polarization included, when  $Z \gg 1$  and  $\alpha = 0$  for unpolarized current, the conductance reduces to

$$\propto |(E + i\Gamma) / \sqrt{(E + i\Gamma)^2 - \Delta^2}|, \text{ precisely the Dynes result for tunneling with inelastic scattering}$$

effects [30]. Thus, our unified model in three limiting cases reproduces the BTK model, the Mazin model and the Dynes model. In addition to the inelastic effects, our results also include spin polarized tunneling effect represented by  $\alpha$ . One can show that except in the purely tunneling regime ( $Z = \infty$ ), the spin polarization can substantially affect the tunneling spectrum.

Next, we discuss the effect of  $Z$ ,  $\alpha$ , and  $\Gamma$  on the probabilities of  $A$ ,  $B$ ,  $C$  and  $D$  when the interface is in equilibrium. As shown in Fig. 1, the three vertical columns are respectively for the effect of  $Z$  ( $\alpha = 0$ ,  $\Gamma = 0$ ),  $\alpha$  ( $Z = 0$ ,  $\Gamma = 0$ ), and  $\Gamma$  ( $\alpha = 0$ ,  $Z = 0$ ). The first column is just the BTK results, whereas the other two columns are the new results. In the first column, as  $Z$  increases,  $A$  is suppressed within the gap resulting a peak at  $E = \Delta$  (Fig. 1a), causing a stronger normal reflection in  $B$  (Fig. 1b), with no quasi-particles inside the gap so the transmission probabilities  $C$  (Fig. 1c) and  $D$  (Fig. 1d) within the gap are zero. Outside the gap, the transmitted probability without branch crossing  $C$  decreases for increasing  $Z$ , because electrons are reflected back by the barrier.

The effect of increasing  $\alpha$  for  $\Gamma = 0$  and  $Z = 0$  is shown in the second column of Fig. 1. The reason for using  $\alpha = 0.0, 1.16, 2.0, 3.46$ , and  $100$  will be discussed later. As  $\alpha$  increases,  $A$

suppresses (Fig. 1e) and  $B$  increases (Fig. 1f). At  $\alpha = 0$ , we have  $A = 1$  and  $B = 0$ , whereas at  $\alpha = 100$ ,  $A \approx 0$  and  $B \approx 1$ . This means that all the electrons are reflected back when  $\alpha$  is large. Inside the gap, both  $A$  and  $B$  remain unchanged. Furthermore,  $\alpha$  has no effect ( $\alpha = 0$  or  $\alpha = 100$ ) on  $C$  (Fig. 1g), strikingly different from the effect of  $Z$  (Fig. 1c). No quasi-particles exist inside gap, thus  $C = D = 0$  for  $E < \Delta$ . When  $E > \Delta$ , most electrons go into the superconductor on the same side of the Fermi surface. However, as  $\alpha$  increases, the probability of branch crossing  $D$  increases outside the gap, as shown in Fig. 1h.

With inelastic scattering, electrons can be scattered into the superconductor as quasi-particles, thus there are transmitted probabilities  $C$  and  $D$  even for  $E < \Delta$  (Fig. 1k). The effect of  $Z$ ,  $\alpha$ , and  $\Gamma$  on probabilities is very different. The  $\Gamma$  factor affects probabilities mostly at the gap (Fig. 1i), while the effect of  $Z$  is mostly at  $E = 0$  (Fig. 1a and 1b) and  $\alpha$  uniformly affects  $A$  and  $B$  within the gap (Fig. 1e and 1f). One notes that both  $Z$  and  $\Gamma$  but not  $\alpha$  have strong effects on  $C$  and  $D$ .

So far we have discussed the effects of spin polarization, inelastic scattering and interfacial scattering in equilibrium. An actual AR experiment is driven to nonequilibrium by a bias voltage. Assuming ballistic transport, the normalized conductance spectrum of an interface with a bias voltage  $V$  is,

$$R_{NN} \frac{dI}{dV} \Big|_{NS} = \frac{Z^2 + 1}{k_B T} \int_{-\infty}^{\infty} \frac{e^{\frac{E - eV - \mu}{k_B T}}}{\left(1 + e^{\frac{E - eV - \mu}{k_B T}}\right)^2} [1 + A(E) - B(E)] dE \quad (1)$$

where  $1/R_{NN} \equiv (1 + Z^2)/(2N(0)e^2 v_F A_S)$ . Coefficients  $A(E)$  and  $B(E)$  are the probabilities listed in Table I.

Previously, since only the coefficients at the limits of purely polarized and unpolarized current have been calculated, the conductance for a partial polarized current has been assumed as a linear combination of the these two extreme cases with  $P_l$  as the coefficient,

$$R_{NN} \frac{dI}{dV} \Big|_{NS} = \frac{Z^2 + 1}{k_B T} \int_{-\infty}^{\infty} \frac{e^{\frac{E - eV - \mu}{k_B T}}}{\left(1 + e^{\frac{E - eV - \mu}{k_B T}}\right)^2} \{ (1 - P_l)[1 + Au(E) - Bu(E)] + P_l[1 + Ap(E) - Bp(E)] \} dE, \quad (2)$$

where  $Au$ ,  $Bu$ ,  $Ap = 0$ , and  $Bp$  are respectively Andreev and normal reflection for purely unpolarized [27] and polarized current [28].

Unique to our new unified model,  $P$  is related to  $\alpha$ , although not  $\alpha$  itself for  $\alpha$  is without limit. In AR with an ideal interface ( $Z = 0$  and  $\Gamma = 0$ ), only the number of minority spins limits the conductance within the gap. The measured spin polarization should be exactly  $1 - A$ , the total probability without AR for an ideal interface. However, while the AR probability  $A$  can be significantly affected by  $Z$  and  $\Gamma$  the *intrinsic* spin polarization of the material in question must remain independent of  $Z$  and  $\Gamma$ . Therefore, the determined spin polarization by the AR method is  $P = 1 - A(Z = \Gamma = 0)$ . From Table I,  $P = 1 - A(Z = \Gamma = 0) = \alpha^2 / (\alpha^2 + 4)$ , a key result of our model that defines the spin polarization  $P$  in terms of  $\alpha$  alone. When  $\alpha = 0$ ,  $P = 0$  while  $P = 1$  for  $\alpha \rightarrow \infty$ . Actually, for  $\alpha = 100$ ,  $P = 0.9996$  is already close to full polarization.

Next, we discuss the effects of  $\alpha$ ,  $\Gamma$  and  $Z$  on AR spectra of both models at 0 K. The normalized conductance curves for various  $\alpha$ 's and  $P_l$ 's are illustrated in Fig. 2. Conductance spectra with  $\alpha = 0.0, 1.16, 2, 3.46, 100$  of the present model of eq. (1) shown by the solid curves are compared with those with  $P_l = 0.0, 0.25, 0.5, 0.75, 1.0$  of the linear model of eq. (2) shown by the dashed curves. For either  $P_l = 0$  and  $P_l = 1$ , the two models are exactly the same since there is only one term in the linear model. Also, if there is no interfacial scattering ( $Z = 0$ ), the



two models have the same results. However, when  $Z \neq 0$ , even a small  $Z = 0.25$  causes noticeable difference between the two models as shown in Fig. 2c and 2d. The difference occurs mostly within the gap. When there are both inelastic and interfacial scattering with  $\Gamma = 0.1$ ,  $Z = 0.25$ , the spectra are similar as those shown in Fig. 2(c) except that they are smoothened (Fig. 2d).

Previously, the AR spectroscopy results analyzed using the linear model generally shows the  $P_I \sim Z$  behavior, which could not be accounted for by any model [32]. In our unified model,  $P = \alpha^2/(\alpha^2 + 4)$ , which is *independent of*  $Z$  and  $\Gamma$ . Our analysis can therefore be used track the *genuine physical* effect of  $Z$  and  $\Gamma$  on  $P$ . Since eq. (1) and eq. (2) describe the same conductance at a  $N/S$  interface, we can equate the two. For  $Z = 0$  and  $\Gamma = 0$ , one finds that  $P_I$  is simply  $\alpha^2/(\alpha^2 + 4)$ , the same as in our model. But if  $Z \neq 0$ ,  $P_I$  depends on other parameters such as  $Z$ ,  $\Gamma$ ,  $T$ . Since both models give the same conductance at  $V = \Delta/e$ , we calculate the dependence of  $P_I$  on  $Z$  for three  $P_I$  values (0.5, 0.75, 0.95 at  $Z = 0$ ) with  $\Gamma = 0$  for  $T = 1.5\text{K}$  and  $4.2\text{K}$ , as illustrated in Fig. 3. As  $Z$  increases,  $P_I$  inevitably decreases just as experimentally observed. The detailed dependence on  $Z$  is more involved, but broadly consistent with  $P_I \sim Z$ . Needless to say, this dependence of  $P_I$  on  $Z$  and  $\Gamma$  is *entirely spurious* for a spin-inert interface; in contrast, our  $P$  does not change at all (Fig. 3). Importantly, at  $Z = 0$ , both models give the *same* spin polarization. Previously, we have extracted intrinsic spin polarization by extrapolating to  $Z = 0$  [14, 18, 19, 22, 24] and, in retrospect, our unified model validates this approach.

In the following, we apply our unified model to some experimental data and compare the results with that from the linear model. The Andreev spectra are obtained from Nb tips in contact with amorphous  $\text{Co}_{40}\text{Fe}_{40}\text{B}_{20}$  thin films made by magnetron sputtering. Over 30 Andreev spectra were obtained with various contact resistances ( $R_C$ ) from  $143\ \Omega$  to  $10\ \Omega$ . Two of the

representative spectra with  $R_C = 128 \, \Omega$  and  $11 \, \Omega$  are shown in Fig. 4 as open circles. The solid and the dashed lines are the best fit using our model and the linear model respectively. Both models give a reasonable fit to the data with the  $P$  values obtained from our model (solid dots) and the linear model (open squares), shown in Fig. 4(e). The decrease of  $P$  is due to the spin-flip scattering of the interface thus our model can be used to determine the intrinsic  $P \sim Z$  relation. We have found our unified model provides a more accurate fit to the superconducting gap  $\Delta$ .

In summary, we present a unified, and most general to date, model of Andreev reflection at an F/S interface of a spin-polarized current quantum mechanically that includes effects due to spin polarization, inelastic scattering, and interfacial scattering. The spin polarization is naturally included instead of assuming a linear combination of unpolarized and polarized currents as in previous models. Our formalism reduces to the well-known BTK model, the Mazin model, and the Dynes model in three limiting cases. The new formalism can address the effects of spin polarization, inelastic and interfacial scattering on all the probabilities involved in Andreev reflection process and also provides significantly better description of the experimental data with more reliable parameters extracted. We also show that the polarization results previously obtained from analyses using the linear model are still valid but only in the limit of negligible interfacial scattering.

## Acknowledgements

This work was supported in part by NSF DMR05-20491 and the IQM, under Grant No. DE-FG02-08ER46544 by the U.S. DoE, Office of Basic Energy Sciences, Division of Materials Sciences and Engineering.

## Reference

\* In memoriam, Z. Tesanovic.

- 1 R. L. Long, Jr., V. W. Hughes, J. S. Greenberg, I. Ames, and R. L. Christensen, Phys. Rev. **138**, A1630 (1965).
- 2 E. Kisker, W. Gudat, E. Kuhlmann, R. Clauberg, and M. Campagna, Phys. Rev. Lett. **45**, 2053 (1980).
- 3 J. S. Moodera and G. Mathon, J. Magn. Magn. Mater. **200**, 248 (1999).
- 4 D. J. Monsma and S. S. P. Parkin, Appl. Phys. Lett. **77**, 720 (2000).
- 5 J. M. D. Teresa, A. Barthelemy, A. Fert, J. P. Contour, F. M., P. Seneor, Science **286**, 506 (1999).
- 6 S. K. Upadhyay, A. Palanisami, R. N. Louie, and R. A. Buhrman, Phys. Rev. Lett. **81**, 3247 (1998).
- 7 R. J. Soulen, Jr., J. M. Byers, M. S. Osofsky, B. Nadgorny, T. Ambrose, S. F. Cheng, P. R. Broussard, C. T. Tanaka, J. Nowak, J. S. Moodera, A. Barry, and J. M. D. Coey, Science **282**, 85 (1998).
- 8 G. J. Strijkers, Y. Ji, F. Y. Yang, C. L. Chien, and J. M. Byers, Phys. Rev. B **63**, 104510 (2001).
- 9 B. Nadgorny, R. J. Soulen, Jr., M. S. Osofsky, I. I. Mazin, G. Laprade, R. J. M. van de Veerdonk, A. A. Smits, S. F. Cheng, E. F. Skelton, and S. B. Qadri, Phys. Rev. B **61**, R3788 (2000).
- 10 B. Nadgorny, I. I. Mazin, M. Osofsky, R. J. Soulen, Jr., P. Broussard, R. M. Stroud, D. J. Singh, V. G. Harris, A. Arsenov, and Y. Mukovskii, Phys. Rev. B **63**, 184433 (2001).
- 11 R. J. Soulen, Jr., M. S. Osofsky, B. Nadgorny, T. Ambrose, P. Broussard, S. F. Cheng, J. Byers, C. T. Tanaka, J. Nowack, J. S. Moodera, G. Laprade, A. Barry, and M. D. Coey, J. Appl. Phys. **85**, 4589 (1999).
- 12 B. Nadgorny, M. S. Osofsky, D. J. Singh, G. T. Woods, R. J. Soulen, Jr., M. K. Lee, S. D. Bu, and C. B. Eom, Appl. Phys. Lett. **82**, 427 (2003).
- 13 J. S. Parker, S. M. Watts, P. G. Ivanov, and P. Xiong, Phys. Rev. Lett. **88**, 196601 (2002).
- 14 Y. Ji, G. J. Strijkers, F. Y. Yang, and C. L. Chien, Phys. Rev. B **64**, 224425 (2001).
- 15 R. Panguluri, G. Tsoi, B. Nadgorny, S. H. Chun, N. Samarth, and I. I. Mazin, Phys. Rev. B **68**, 201307(R) (2003).

- 16 R. Panguluri, B. Nadgorny, T. Wojtowicz, W. L. Lim, X. Liu, and J. K. Furdyna, Appl. Phys. Lett. **84**, 4947 (2004).
- 17 T. Y. Chen, C. L. Chien, and C. Petrovic, Appl. Phys. Lett., **91**, 142505 (2007).
- 18 S. X. Huang, T. Y. Chen, and C. L. Chien, Appl. Phys. Lett., **92**, 242509 (2008).
- 19 T. Y. Chen, S. X. Huang, and C. L. Chien, Phys. Rev. B **81**, 214444 (2010).
- 20 P. Kharel, P. Thapa, P. Lukashev, R. F. Sabirianov, E. Y. Tsymbal, D. J. Sellmyer, and B. Nadgorny, Phys. Rev. B **83**, 024415 (2011).
- 21 A. D. Naylor, G. Burnell, and B. J. Hickey, Phys. Rev. B **85**, 064410 (2012).
- 22 Y. Ji, C. L. Chien, Y. Tomioka, and Y. Tokura, Phys. Rev. B **66**, 012410 (2002).
- 23 L. Wang, K. Umemoto, R. M. Wentzcovitch, T. Y. Chen, C. L. Chien, J. G. Checkelsky, J. C. Eckert, E. D. Dahlberg, and C. Leighton, Phys. Rev. Lett., **94**, 056602 (2005).
- 24 J. S. Parker, S. M. Watts, P. G. Ivanov, and P. Xiong, Phys. Rev. Lett. **88**, 196601 (2002).
- 25 Y. Ji, G. J. Strijkers, F. Y. Yang, C. L. Chien, J. M. Byers, A. Anguelouch, G. Xiao, and A. Gupta, Phys. Rev. Lett. **86**, 5585 (2001).
- 26 T. Y. Chen, Z. Tesanovic, R. H. Liu, X. H. Chen, and C. L. Chien, Nature **453**, 1224 (2008).
- 27 G. E. Blonder, M. Tinkham, and T. M. Klapwijk, Phys. Rev. B **25**, 4515 (1982).
- 28 I. I. Mazin, A. A. Golubov, and B. Nadgorny, J. Appl. Phys. **89**, 7576 (2001).
- 29 G. T. Woods, R. J. Soulen, Jr., I. I. Mazin, B. Nadgorny, M. S. Osofsky, J. Sanders, H. Srikanth, W. F. Egelhoff, and R. Datla, Phys. Rev. B **70**, 054416 (2004).
- 30 R. C. Dynes, J. P. Garno, G. B. Hertel, and T. P. Orlando, Phys. Rev. Lett. **53**, 2437 (1984).
- 31 A. Plecenik, M. Grajcar, Š. Beňačka, P. Seidel and A. Pfuch, Phys. Rev. B **49**, 10016 (1994).
- 32 C. H. Kant, O. Kurnosikov, A. T. Filip, P. LeClair, H. J. M. Swagten, and W. J. M. de Jonge, Phys. Rev. B **66**, 212403 (2002).

Table I Probabilities of of an F/S interface:  $A = aa^*$  gives the probability of Andreev reflection,  $B = bb^*$  of ordinary reflection,  $C = cc^*(\tilde{u}\tilde{u}^* - \tilde{v}\tilde{v}^*)$  of transmission without branch crossing, and  $D = dd^*(\tilde{u}\tilde{u}^* - \tilde{v}\tilde{v}^*)$  of transmission with branch crossing.

$$[\tilde{u}^2 = 1 - \tilde{v}^2 = (1 + \sqrt{(|E| + i\Gamma)^2 - \Delta^2} / (|E| + i\Gamma)) / 2, \quad \gamma = \tilde{u}^2(-i + Z)(\alpha + 2i + 2Z) - \tilde{v}^2 Z(\alpha + 2Z),$$

$$\gamma_1 = \tilde{u}^2 + (\tilde{u}^2 - \tilde{v}^2)Z^2, \quad \gamma_2 = \tilde{u}^2(-i + Z) - \tilde{v}^2 Z^2]$$

	$a$	$b$	$c$	$d$
This work	$\frac{2\tilde{u}\tilde{v}}{\gamma}$	$\frac{-\tilde{u}^2 Z(\alpha + 2i + 2Z) + \tilde{v}^2(i + Z)(\alpha + 2Z)}{\gamma}$	$\frac{-i\tilde{u}(\alpha + 2i + 2Z)}{\gamma}$	$\frac{i\tilde{v}(\alpha + 2Z)}{\gamma}$
$\alpha = 0$ BTK	$\frac{\tilde{u}\tilde{v}}{\gamma_1}$	$-\frac{(\tilde{u}^2 - \tilde{v}^2)(i + Z)Z}{\gamma_1}$	$\frac{\tilde{u}(1 - iZ)}{\gamma_1}$	$\frac{i\tilde{v}Z}{\gamma_1}$
$\alpha = \infty$ Mazin	0	$\frac{-\tilde{u}^2 Z + \tilde{v}^2(i + Z)}{\gamma_2}$	$\frac{-i\tilde{u}}{\gamma_2}$	$\frac{i\tilde{v}}{\gamma_2}$

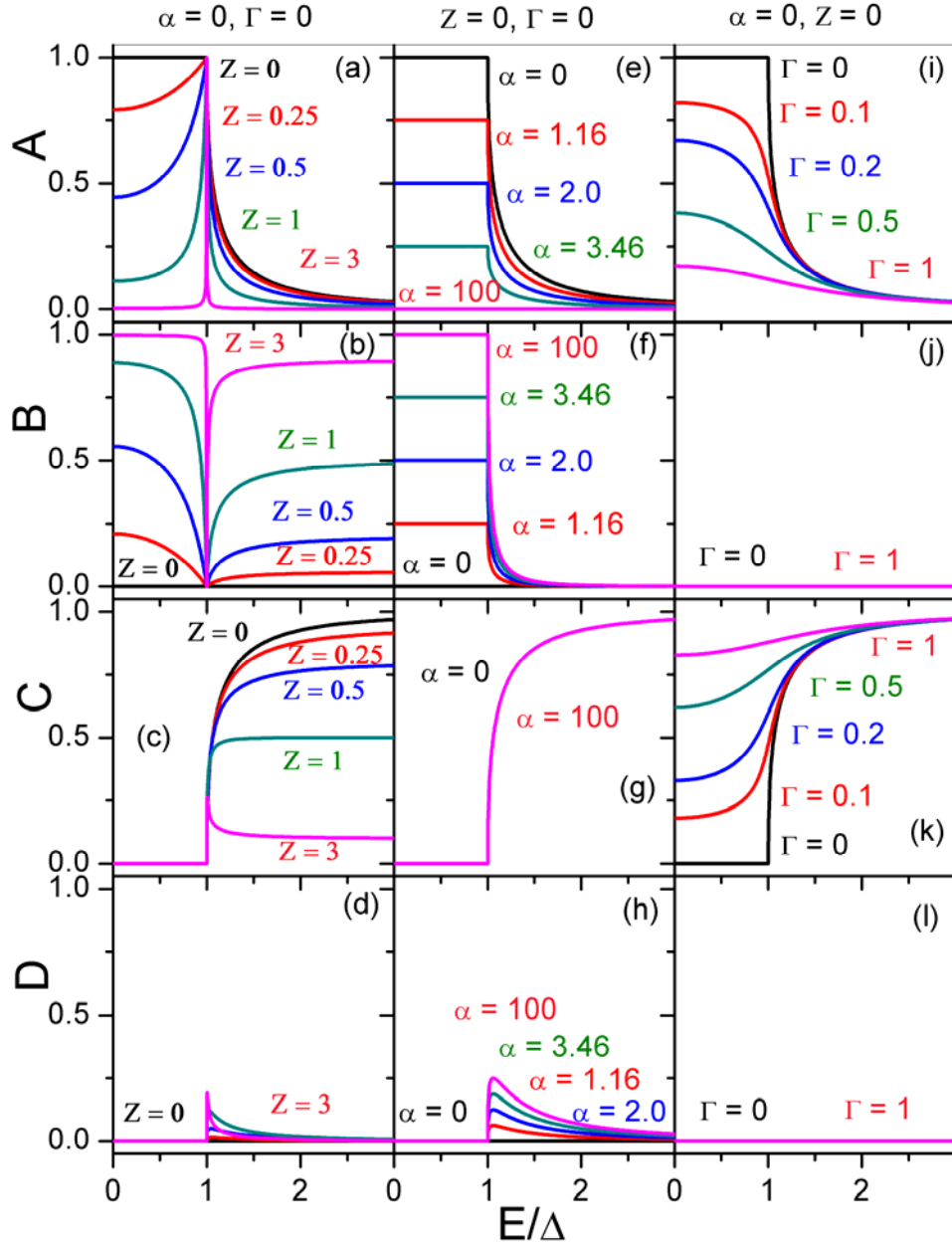


Fig. 1 Effect of polarization  $\alpha$ , interfacial scattering  $Z$ , and inelastic scattering  $\Gamma$  on transmission and reflection probabilities  $A$ ,  $B$ ,  $C$  and  $D$  for (a-d)  $Z = 0, 0.25, 0.5, 1, 3$ , (e-h)  $\alpha = 0, 1.16, 2, 3.46, 100$ , and (i-l)  $\Gamma = 0, 0.1, 0.2, 0.5, 1$ .

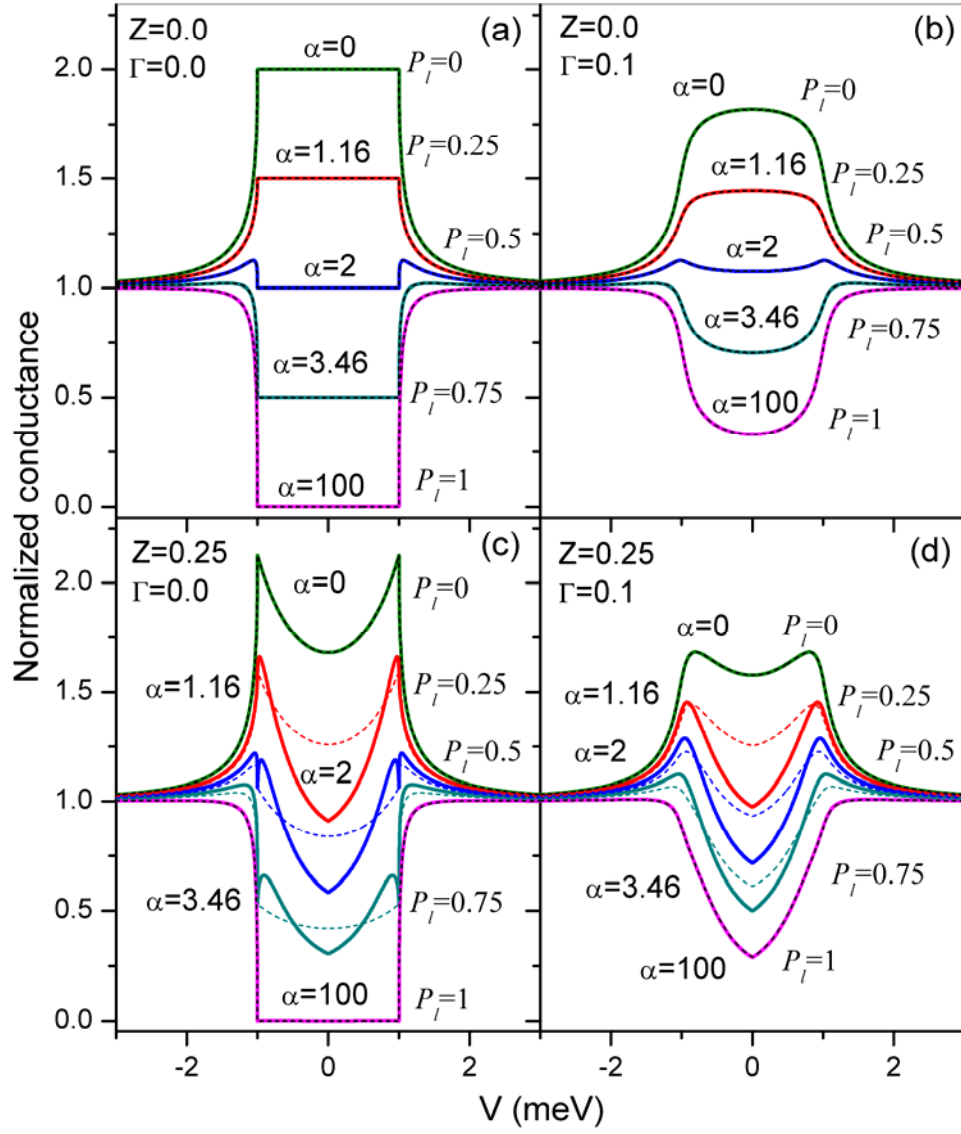


Fig. 2 Effect of spin polarization on conductance spectra from this model (solid lines) and the linear model (dashed lines) for various  $\alpha=0, 1.16, 2, 3.46, 100$  and  $P_l=0, 0.25, 0.5, 0.75, 1$  with (a)  $Z = \Gamma = 0$ , (b)  $Z = 0, \Gamma = 0.1$ , (c)  $Z = 0.25, \Gamma = 0$ , and (d)  $Z = 0.25, \Gamma = 0.1$ .

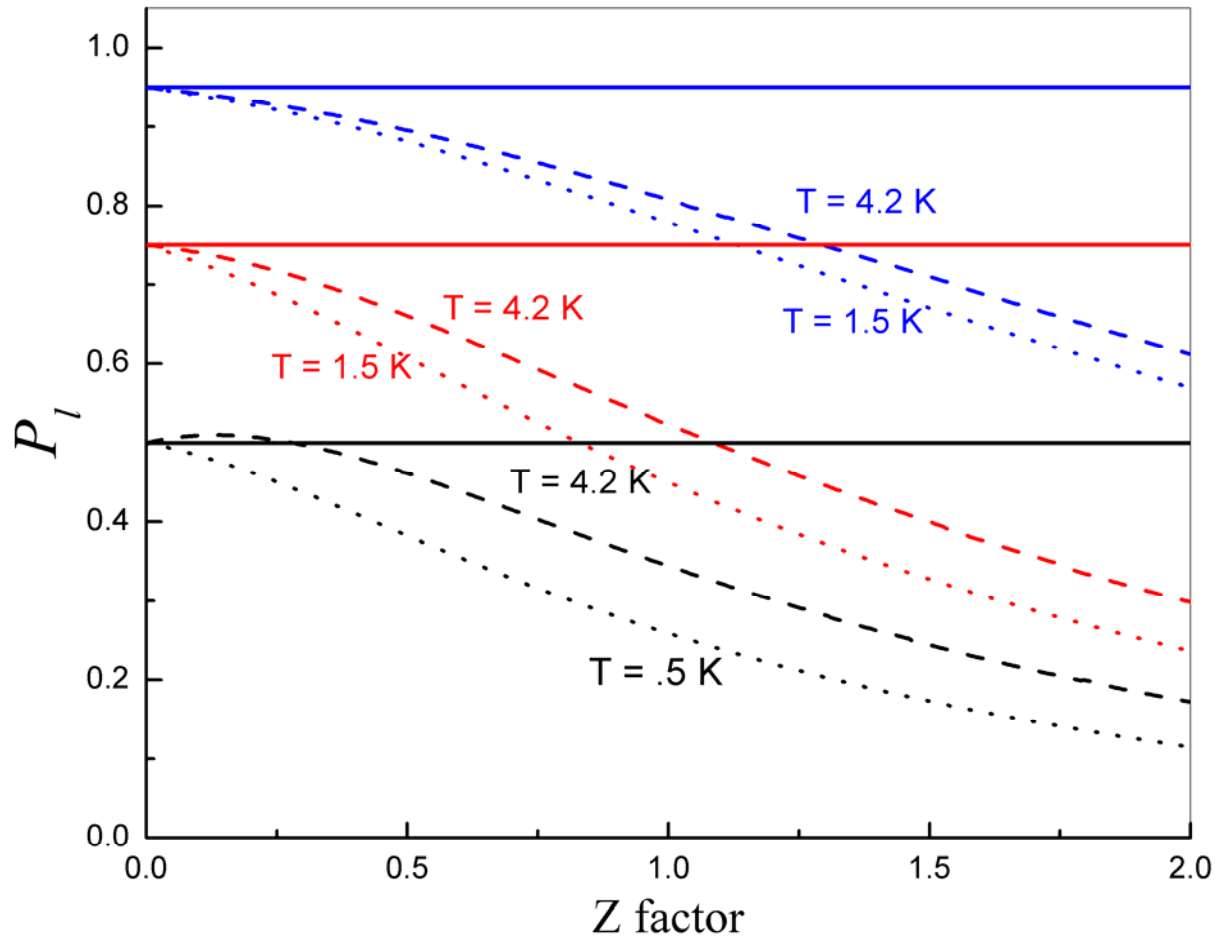


Fig. 3 Calculated spin polarization ( $P_l = 0.5, 0.75$ , and  $0.95$  at  $Z = 0$ ) of the linear combination model as a function of  $Z$  ( $\Gamma = 0$  and  $V = \Delta/e$ ) at  $1.5$  K (dot line) and  $4.2$  K (dashed lines). Solid lines are spin polarization from this model.



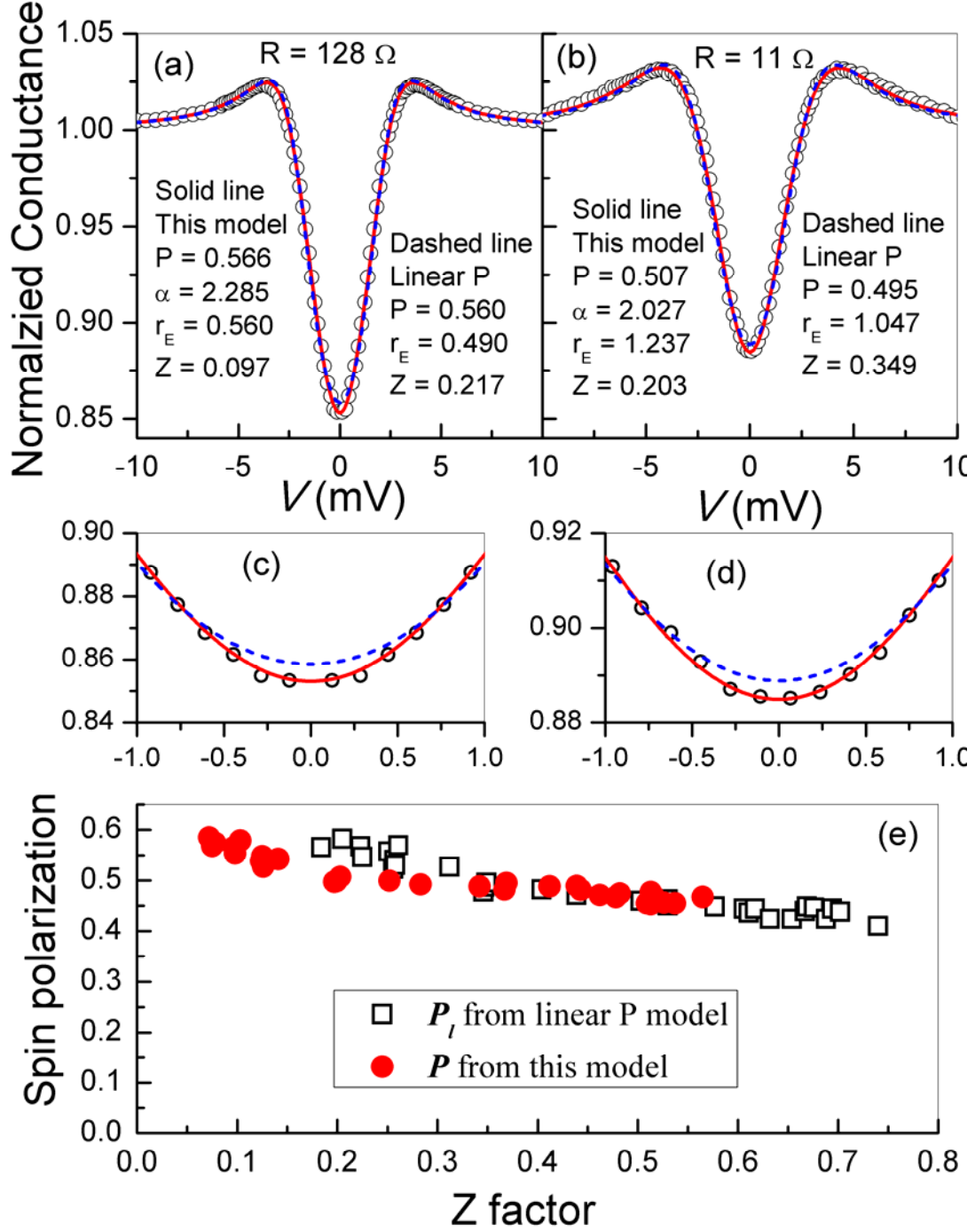


Fig. 4 Two Andreev spectra (open circles) of Nb/Co<sub>40</sub>Fe<sub>40</sub>B<sub>20</sub> contacts with  $R_C = 128 \Omega$  (a) and  $11 \Omega$  (b) analyzed by this model (solid) and the linear model (dashed) with  $T = 4.25$  K,  $\Delta = 1.42$  meV fixed as experimental values and  $\Gamma = 0$ , (e) determined spin polarization value as a function of  $Z$ . Additional resistance  $r_E$  is addressed in ref. 19.